CrossMark

ORIGINAL PAPER

Modeling evapotranspiration in a spring wheat from thermal radiometry: crop coefficients and *E/T* partitioning

J. M. Sánchez[1] · R. López-Urrea[2] · C. Doña[3] · V. Caselles[3] · J. González-Piqueras[4] · R. Niclòs[3]

Abstract Wheat is one of the crops occupying the largest areas in the world (218 million ha in 2013). Understanding the land–atmosphere energy exchanges over these croplands becomes important not only for agronomy but also for climatic and meteorological aspects. This study continues previous work on the estimation of actual evapotranspiration (ET) and the assessment of crop coefficients of sorghum, sunflower, or canola. Two variations of a simple two-source energy balance (STSEB) approach were used in combination with land surface temperature measurements to calculate hourly and daily values of surface fluxes and actual ET. An experiment was carried out during the spring season of 2014 in Las Tiesas experimental farm in Barrax, Spain. Soil and canopy temperature components together with meteorological variables and biophysical parameters were measured from planting to senescence. Comparison to lysimeter measurements showed calculation errors of ± 0.11 mm h^{-1} and ± 0.8 mm day^{-1} for hourly and daily ET values, respectively, whereas an underestimation no >4 % resulted from the entire campaign. Partition between soil and canopy components yielded a ratio of evaporation (*E*) to transpiration (*T*) of 36–64 %, respectively, for the total growing season. Dual crop coefficients were also calculated and compared to those proposed by FAO-56. Although separate *E* and *T* measurements were not available, similar results between the STSEB and FAO-56 models demonstrate the utility of the STSEB for investigating management strategies aimed at increasing crop water use efficiency.

Introduction

Better management of water resources becomes critical for sustainable development as a consequence of increasing global water demand and severity of droughts. Nowadays, crop irrigation remains the main source of water consumption. This work focuses on wheat, which is one of the most important crops worldwide, covering a total area of 218 million ha in 2013. In the European Union (EU), more than 25 million ha was cultivated in the year 2013 with a production of 143.3 million tons, approximately 20 % of world production. Spain is the fifth producing country within the EU, with an area of 2.1 million ha and a production of 7.6 million tons (FAO 2014). Wheat area in Spain has increased almost 20 % in the past 4 years. Castilla y León is the Spanish region with the largest surface area of wheat (around 780,000 ha), while Castilla-La Mancha holds second place with nearly 320,000 ha (MAGRAMA 2014). In this framework, understanding the land–atmosphere energy exchanges over wheat crop becomes important not only for agronomy but also for climatic and meteorological aspects.

✉ J. M. Sánchez
   juanmanuel.sanchez@uclm.es

1. Applied Physics Department, School of Mining and Industrial Engineering, University of Castilla-La Mancha, Plz. Manuel Meca, 1, 13400 Almadén, Spain

2. Instituto Técnico Agronómico Provincial de Albacete and FUNDESCAM, Polígono Industrial Campollano, Avda. 2ª-42 B, 02007 Albacete, Spain

3. Earth Physics and Thermodynamics Department, Faculty of Physics, University of Valencia, C/Dr. Moliner, 50, 46100 Burjassot, Spain

4. Applied Physics Department, School of Agronomic Engineering and IDR, University of Castilla-La Mancha, Av. España s/n, 02071 Albacete, Spain

Springer

The most common approach widely used for calculating the soil water balance and estimating crop water requirement is the FAO-56 method (Allen et al. 1998). According to FAO-56, crop actual evapotranspiration (ET) is estimated by the combination of a reference evapotranspiration (ET_o) and crop coefficients. There are two different FAO-56 approaches: single and dual crop coefficients. The single crop coefficient approach is used to express both plant transpiration and soil evaporation combined into a single crop coefficient (K_c). The dual crop coefficient approach uses two coefficients to separate the respective contribution of plant transpiration (K_{cb}) and soil evaporation (K_e), each by individual values (Allen et al. 1998). This dual crop coefficient technique can improve the accuracy of ET estimation although it requires calibration of the coefficients. This technique has been widely applied and explored under a variety of climatic conditions worldwide (Hunsaker et al. 2005; Williams and Ayars 2005; López-Urrea et al. 2009, 2012, 2014; Campos et al. 2010; Howell et al. 2012; Zhang et al. 2013; Ghamarnia et al. 2014). All these authors agree that crop coefficient values taken from the literature may serve as a starting point for irrigation scheduling, but corrections to these initial values become necessary to adjust to local conditions since considerable errors may occur due to their empirical nature. With this aim, many authors have shown the possibility of using remote sensing measurements to estimate crop water requirements and then improve irrigation scheduling and water productivity. Focusing on wheat, López-Urrea et al. (2009) determined crop coefficient of this crop in the semiarid climatic conditions of central Spain, using a weighing lysimeter. These authors showed good agreement with the values proposed by FAO-56 and published by other authors. Gontia and Tiwari (2010) generated monthly crop coefficient maps of wheat croplands in India from vegetation indexes information and used those to estimate ET maps. Zhao et al. (2013) adopted the dual crop coefficient approach to simulating the soil water balance in winter wheat in the North China Plain (NCP) and tested the SIMDualKc model. Gao et al. (2014) calibrated this model in the same Chinese region with data from a winter wheat but with subsurface drip irrigation. Shahrokhnia and Sepaskhah (2013) used weighing lysimeters to evaluate and calibrate the values proposed by FAO for the daily crop coefficient and ET of wheat in the Fars province, Iran. Yang et al. (2014) used a complementary relationship model coupled with an evaporative fraction (EF) approach to estimating ET of winter wheat in the NCP, based on meteorological data and a high-resolution IKONOS image. Farg et al. (2012) estimated crop coefficients for wheat in the south Nile Delta of Egypt using vegetation indices derived from SPOT-4 satellite data. Zhang et al. (2015) used MODIS data with an energy balance ET model (EBEM) to estimate daily ET in the NCP, and the results were compared to lysimeter measurements.

The combination of two-source energy balance with local radiometric temperatures has been shown to effectively estimate actual ET values under a variety of crops and environmental conditions (French et al. 2007; Sánchez et al. 2008, 2011; Colaizzi et al. 2012; Kustas et al. 2012). The main limitation to the operational application of this technique at a regional scale is the retrieval of land surface temperature from satellite data with the sufficient spatial and temporal resolutions, especially in those agricultural areas composed of cropped fields smaller than 1 ha. Nowadays, none of the operating satellites offer the combination of spatial and temporal resolution of thermal infrared (TIR) bands needed for these applications. However, significant progress is being made in disaggregation techniques for downscaling information of TIR bands using higher-resolution visible/near-infrared (VIS/NIR) bands (Agam et al. 2007; Bindhu et al. 2013; Gao et al. 2012). This is expected to bring the opportunity to use some operating satellites such as SPOT, DEIMOS, or FORMOSAT, and others coming soon, such as the promising SENTINEL-2, which do not include TIR bands but will offer high-resolution VIS/NIR images (10–20 m). In a recent paper, Sánchez et al. (2014) applied this technique to separate evaporation (E) and transpiration (T) components, and those were used to predict dual crop coefficients for sunflower and canola crops. A new experiment was carried out in the spring growing season of 2014 in a wheat field located in a semiarid region of central Spain. The methodology and experimental setup were similar to those already described in Sánchez et al. (2014), so the aim of this work is presenting the new results for a wheat crop and reinforcing the potential of thermal infrared measurements as an alternative technique to FAO-56 for the evaluation and partitioning of ET into E and T components. This can be also considered a useful tool for the local adjustment of the FAO-56 crop coefficients.

Materials and methods

This experiment was carried out in "Las Tiesas" experimental farm (2º5′W, 39º3′N, 695 m a.s.l) located in the semiarid, temperate Mediterranean province of Albacete (central Spain) from February to June 2014. The study site is a 100 m × 100 m field with a weighing lysimeter (2.7 m long, 2.3 m wide, and 1.7 m deep) installed in the center of the plot characterized by a resolution of 0.04 mm equivalent water depth. Weighing lysimeters are presently the most accurate method to measure ET (Howell et al. 1995). The soil is classified as *Petrocalcic Calcixerepts*. Average soil depth of the experimental plot is 40 cm and is limited by the development of a more or less fragmented petrocalcic horizon. Texture is silty clay loam, with 13 % sand,

Fig. 1 Experimental setup over the lysimeter for DOYs 55 and 129 (*top*), and view of the wheat field conditions for DOYs 153 and 174 (*bottom*)

Fig. 2 The 2014 wheat season phenology showing fractional vegetation cover (P_v) and the canopy height (h). *Marks* correspond to measured values and *lines* represent modeled behavior

49 % silt, and 38 % clay, with a basic pH (8.1). The soil is low in organic matter (1.48 %) and nitrogen (0.10 %) and has a high content of active limestone (12.5 %). For a more comprehensive description of the site and technical features of the lysimeter, see López-Urrea et al. (2006) and Sánchez et al. (2011).

Wheat (*Triticum aestivum* L. cv. ´Califa´) was sowed on February 4 in rows 15 cm apart with a seed population of 550 seeds m^{-2} (Fig. 1). Measurements started on 12 February (DOY 43) and lasted to 30 June (DOY 181). Efforts were made to keep the crop inside the lysimeter at the same growth rate and plant population as the crop outside to minimize edge effects. The whole plot has a permanent sprinkler irrigation system with sprinklers placed on a grid of 15 m × 12.5 m that provide a precipitation rate of 8.6 mm h^{-1}. During the experiment, wheat was irrigated, avoiding water stress conditions at anytime. Fractional vegetation cover (P_v) and crop height were measured weekly, and then modeled for the entire experiment, to monitor crop development (Fig. 2). The fractional vegetation cover (P_v) was determined using a supervised classification technique of digital photographic images with the maximum probability algorithm (Calera et al. 2001), in order to assign the current classes of green vegetation and soil
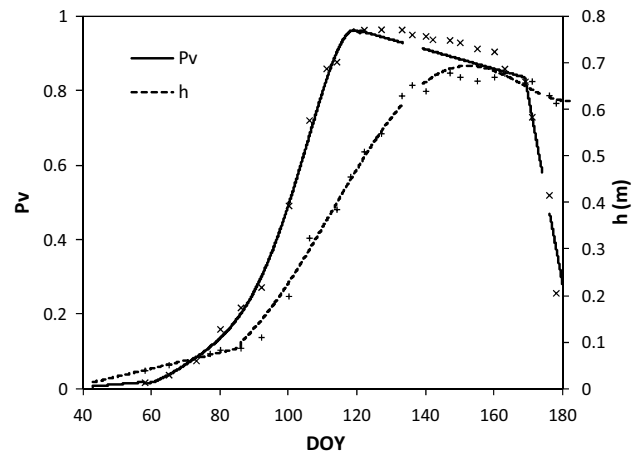
in the image, based on the classic methodology for calculating green plant cover developed by Cihlar et al. (1987). Digital photographs acquired weekly over the lysimeter area were always taken at solar noon and vertically from an approximate height of 2 m above ground. Supervised classification of these digital images was later carried out with the help of the ENVI® computer program. Crop height (h) was measured also weekly, in plant samples from three separate areas, as the distance between ground level and the peak of the plant. Best fitting values for both P_v and h data series were used to reproduce their curves for the entire experiment.

Three Apogee SI-121 thermal infrared radiometers (IRT) (Apogee Instruments, Logan UT, USA) were used in this experiment. These are broadband thermal instruments (8–14 μm) with an accuracy of ±0.2 °C, a 18° field of view, and a valid temperature range from −30 to 65 °C. One was placed at a height of 2 m over the lysimeter spot, looking at the surface with nadir view and measuring the composite target temperature (T_R). A second radiometer was placed at a height of 20 cm directly pointing to the soil between rows (Fig. 1) to measure soil temperature data (T_s). Canopy temperature (T_c) values were inferred from T_R and T_s, using P_v information, as described in Sánchez et al. (2014). This experimental setup avoids limitations in obtaining T_c using IRTs with a near-horizontal view, especially for low values of P_v.

All temperatures were corrected for emissivity and atmospheric effects. At this point, downwelling sky radiance was calculated from sky brightness temperature values measured by a third Apogee radiometer pointing at the sky with an angle of 53°. Values of $\varepsilon_c = 0.987 \pm 0.005$ and $\varepsilon_s = 0.960 \pm 0.013$ were used for this study (Rubio et al. 2003).

Table 1 Mean values of the meteorological variables: air temperature (T_a), relative humidity (H_r), wind speed (u), solar irradiance (S), reference evapotranspiration (ET_0), soil moisture at -10 cm (SM), and cumulated precipitation (Prec.) and irrigation (Irr.), at the wheat plot for the entire experiment

	T_a (°C)	H_r (%)	u (m s^{-1})	S (W m^{-2})	SM (m^3 m^{-3})	Prec. (mm)	Irr. (mm)	ET_0 (mm day^{-1})
February[a]	7.3	60	4.2	134	0.28	8	16	1.9
March	8.8	66	3.9	196	0.28	2	70	2.9
April	13.8	69	3.0	255	0.27	37	46	4.2
May	15.9	60	2.6	302	0.28	5	183	5.3
June	20.1	59	2.4	305	0.25	43	119	5.6

[a] Starting 12 February

Air temperature (T_a) and relative humidity (H_r) were measured using a HMP50 probe (Vaisala Inc., Helsinki, Finland). Wind speed (u) was measured by an anemometer (model A100R, VectorInstruments Ltd., UK). Solar irradiance (S) (model CM14, Kipp & Zonen Delft, Holland) and incoming long-wave radiance (L_{sky}) (model CG2, Kipp & Zonen Delft, Holland) were also measured. Net radiation (R_n) was measured by a NR-Lite sensor (Kipp & Zonen, Delft, The Netherlands) mounted over the lysimeter spot. Soil moisture (SM) was monitored using a capacitance sensor (10HS ECH$_2$O, Decagon Devices Inc., Pullman, WA) at 10 cm depth. All data were stored every 15 min, using a CR-1000 datalogger (Campbell Scientific Inc., Logan, USA), and averaged at hourly scale. Table 1 lists a summary of the mean values of these variables and parameters for the entire experiment.

In this work, a simplified version of the two-source energy balance (STSEB) (Sánchez et al. 2008) was applied to estimate total and separate soil and canopy energy fluxes using the radiometric temperatures, biophysical information, and meteorological data as inputs. A summary of the different equations, parameters, and methodological procedure of the STSEB model is included in the "Appendix." The reader is referred to Sánchez et al. (2008) and (2011) for a more comprehensive description. This approach was conceived to be applied when the radiometric temperatures of both soil and canopy are known or at least one of them together with the composite temperature T_R. However, application of STSEB is also possible when only T_R is available, upon the inclusion of some assumptions as part of the approach, for example an initial calculation of canopy transpiration using the Priestley–Taylor equation (Priestley and Taylor 1972). A scheme of this formulation of the STSEB-T_R model is included in the "Appendix." A test of this version of the model (STSEB-T_R) was carried out, and results were compared to the pure STSEB approach.

Agreement between modeled and measured values of the surface energy fluxes is analyzed in this paper in terms of the parameters of the linear regression adjustment (slope, intercept, and determination coefficient, r^2), the root-mean-squared error (RMSE), and the mean bias error (MBE) (Willmott 1982).

Results and discussion

Comparison between STSEB and STSEB-T_R

Results of the different terms of the energy balance equation were obtained and averaged at an hourly scale, applying both the original STSEB and the modified STSEB-T_R formulations (see "Appendix"). Figure 3 shows the comparison between the two version outcomes. Differences between the two formulations are negligible in terms of net radiation (R_n) and soil heat fluxes (G), with RMSE values lower than 5 W m^{-2}. Some discrepancies arise in terms of the sensible heat flux (H), with a RMSE = 20 W m^{-2}. This absolute error is maintained in ET estimates. However, the non-water-stressed status of this wheat experiment masks this deviation in ET since H is a minor term compared to R_n under these conditions. Nevertheless, a slight underestimation of ET is observed with the STSEB-T_R approach, more evident for large ET values. These results give confidence to the application of the STSEB-T_R scheme in those scenarios where only the composite target temperature is available and non-water-stressed conditions are prevalent. Further adjustments in the Priestley–Taylor approach would be required under different surface and environmental conditions (Colaizzi et al. 2012).

Modeled wheat ET

An accurate estimate of the net radiation is critical for obtaining accurate LE values. Figure 4a shows the comparison between modeled and observed values of R_n. A RMSE value of ± 35 W m^{-2}, corresponding to an average relative error of ± 10 %, was observed for both the original STSEB and the STSEB-T_R calculations. These results are very close to the value of ± 7 % obtained in Zhang
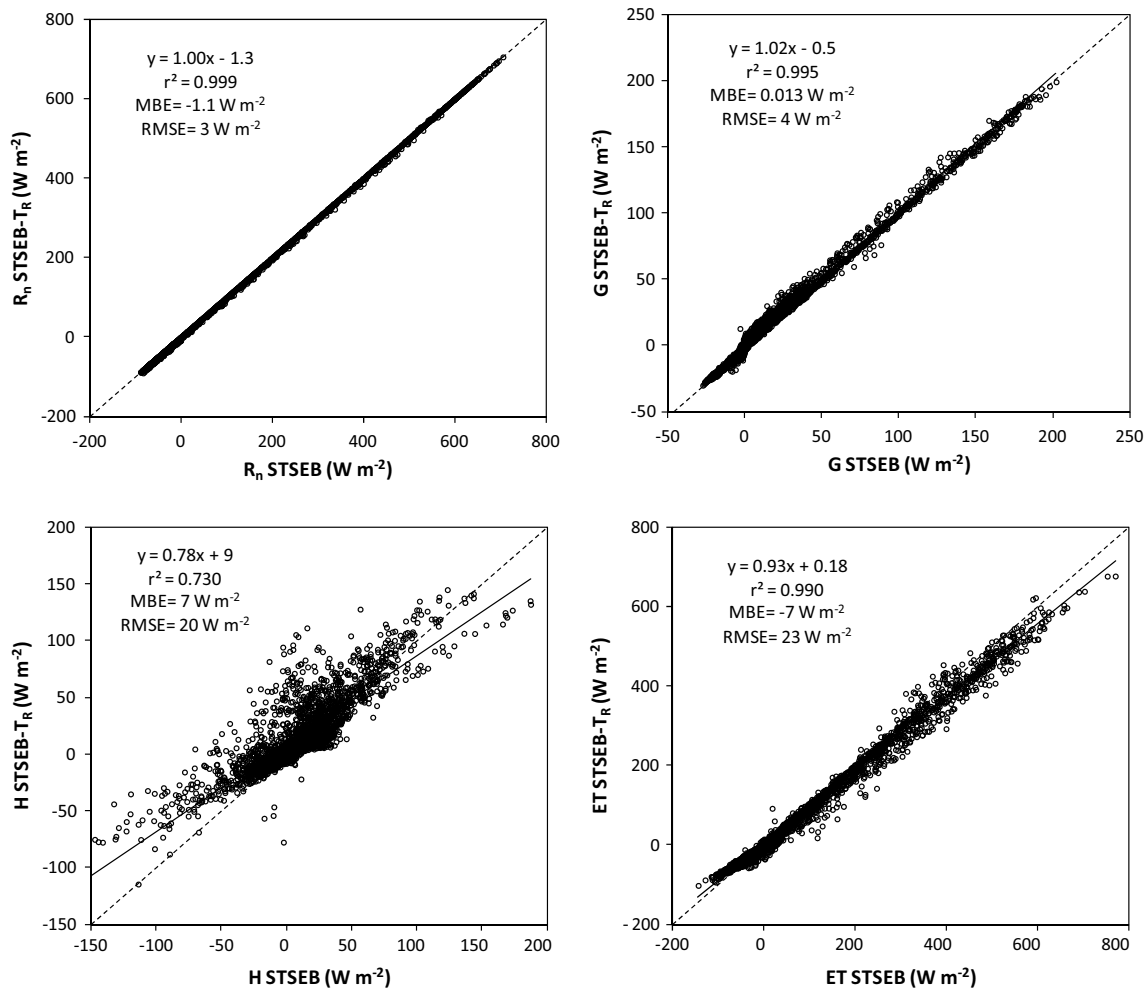
Fig. 3 Comparison of hourly estimates of the different terms of the surface energy balance (R_n, G, H, and ET), using the original STSEB approach and the modified STSEB-T_R formulation

et al. (2015) over wheat. Colaizzi et al. (2012) applied the original TSEB approach, using separate measurements of T_s and T_c, to an irrigated cotton crop and observed a very similar RMSE of ± 30 W m^{-2} in the retrieval of R_n. Very good agreement was observed also by these authors when comparing TSEB and a modified TSEB-T_R formulation (Colaizzi et al. 2012), in terms of R_n estimates.

Hourly values of ET, ranging between -0.2 and 1.2 mm h^{-1}, were compared to lysimeter measurements (Fig. 4b). Using the original STSEB model, a root-mean-square error of ± 0.11 mm h^{-1} was obtained, and the bias was negligible. Similar RMSE $= \pm 0.11$ mm h^{-1}, with an underestimation of -0.03 mm h^{-1} and a slightly larger scatter, resulted from the application of the STSEB-T_R approach. These results are an improvement over Sánchez et al. (2011) and (2014), where RMSE values close to ± 0.20 mm h^{-1} for sunflower and canola, and ± 0.14 mm h^{-1} for sorghum, were observed.

The original STSEB approach will be used hereafter for the rest of the analysis since, as shown above, it seems to reproduce slightly better results than the STSEB-T_R in this work.

The evolution of the daily ET (ET$_d$) values, modeled and measured, is shown in Fig. 5a. Average ET$_d$ value remained below 3 mm day^{-1} until the end of March, peaked 9–10 mm day^{-1} between middle May and middle June, and declined afterward during the grain filling through physiological maturity period. In general, lysimeter ET$_d$ values are well captured by the STSEB model estimates for the entire wheat growing season, except very few days when some rain events occurred and the lysimeter measure had to be recalculated. Following these precipitation events, and very few other weight and calibration verifications, the lysimeter mass data were interpolated using measurements made immediately prior to and immediately following dates that required adjustments. As shown in Fig. 5b,
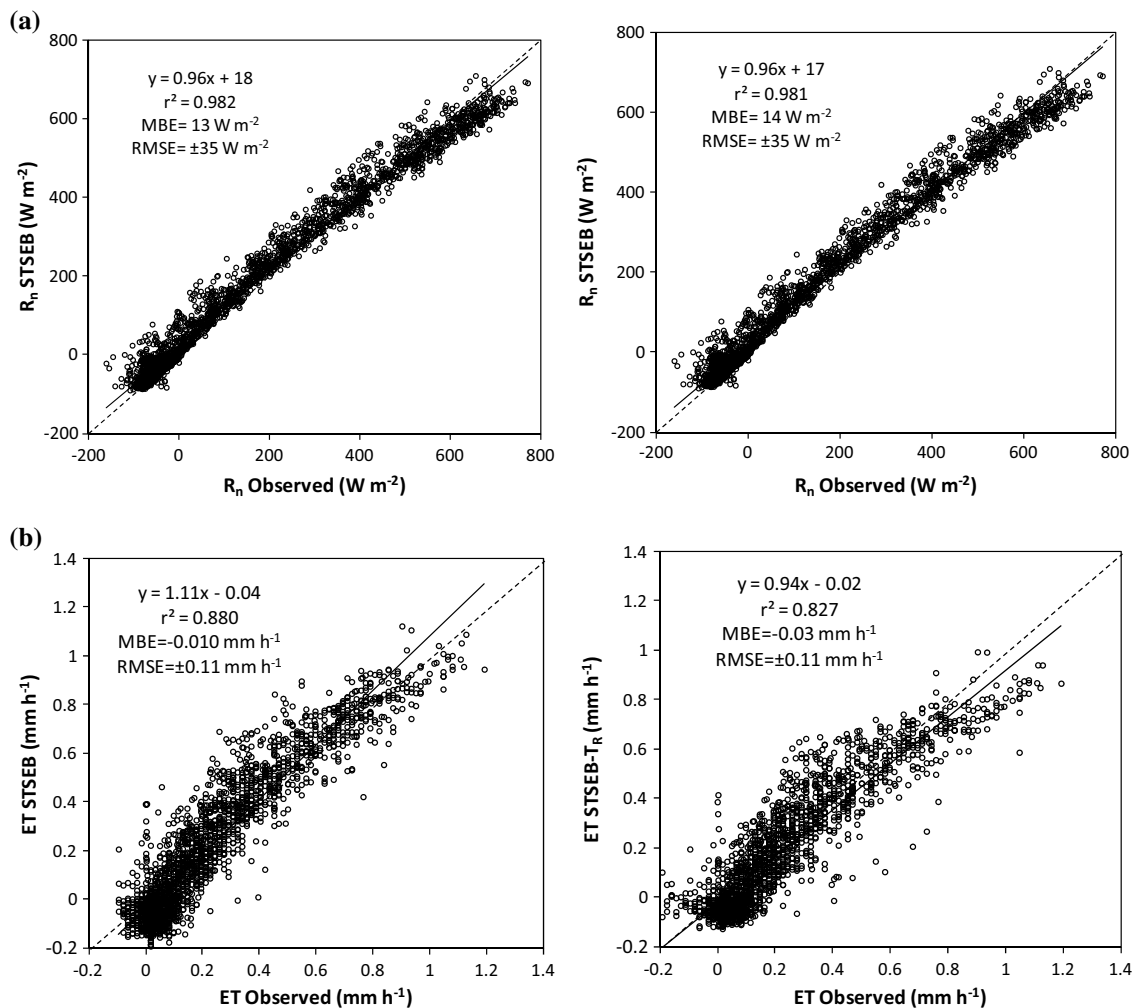
(a)

(b)

Fig. 4 Calculated versus ground-measured hourly variables using the original STSEB approach and the modified STSEB-T_R formulation: **a** net radiation, **b** evapotranspiration

discrepancies were within ± 1.0 mm day^{-1} for more than 85 % of the dataset.

Quantitative analysis of the comparison between modeled and observed daily ET (ET$_d$) shows an average underestimation of 0.18 mm day^{-1} with a RMSE value of ± 0.8 mm day^{-1} and a determination coefficient (r^2) of 0.903 (Fig. 6). Results are again in agreement with those obtained in Sánchez et al. (2011) and (2014), where RMSE values of ± 1.0 mm day^{-1} were observed for sorghum, sunflower, and canola and very close to the RMSE = ± 1.1 mm day^{-1} shown by Colaizzi et al. (2012) in irrigated cotton fields also using weighing lysimeters. These authors pointed out an underestimation of the TSEB early in the season and an overestimation later on, when using direct T_s and T_c measurements. Note that these direct T_c and T_s measurements consider the contribution of the entire canopy and soil, respectively, accounting for sunlit and shaded portions, and this proportion varies with

time of day and canopy structure. Also, some experimental limitations arise when measuring T_c using IRTs with near-horizontal view for low vegetation cover conditions (Colaizzi et al. 2012), resulting in an overestimation of the canopy temperature that yields a subsequent underestimation of ET. Colaizzi et al. (2012) postulated that overestimates of E could be due to model assumptions and T_s measurements not accounting for the whole interrow portion. Late season ET overestimates were also reported by French et al. (2007) for wheat, and they attributed this to leaf senescence. This behavior in the discrepancies is not observed in Fig. 5b. Focusing on wheat, Zhang et al. (2013) compared ET values predicted by their simulation model with those obtained from eddy covariance measurements. Values of RMSE = ± 0.6 mm day^{-1} and r^2 of 0.92 were observed by these authors in a winter wheat. A similar error of RMSE = ± 0.4 mm day^{-1} was shown by Gao et al. (2014) as a result of the comparison between

Fig. 5 a Evolution of modeled and observed daily ET values for the wheat season. Irrigation and rainfall amounts are also included. **b** Daily ET discrepancy (modeled ET–observed ET) over the growing season
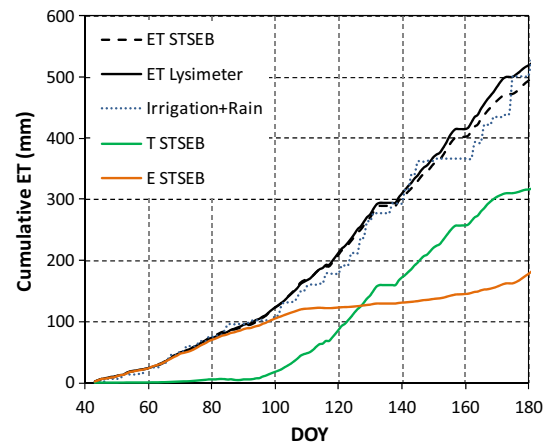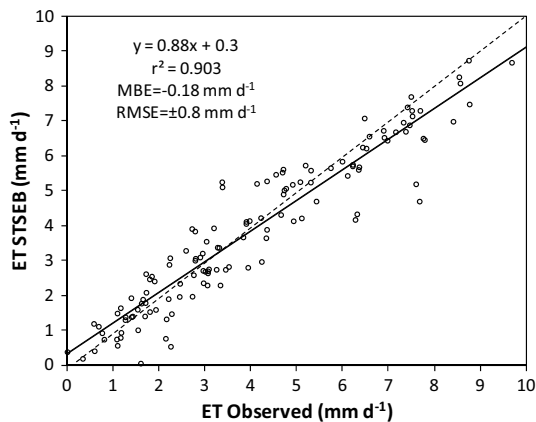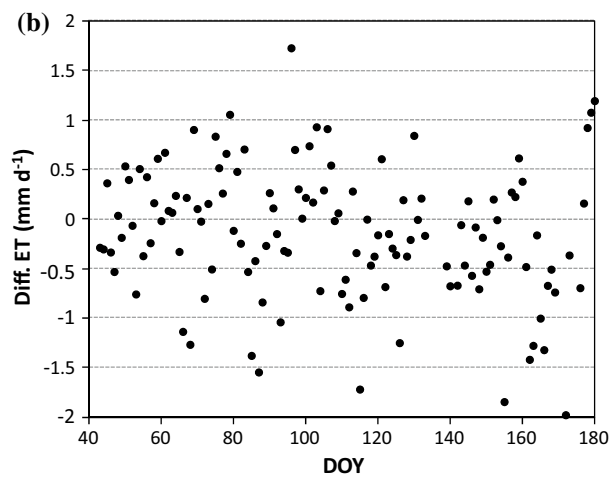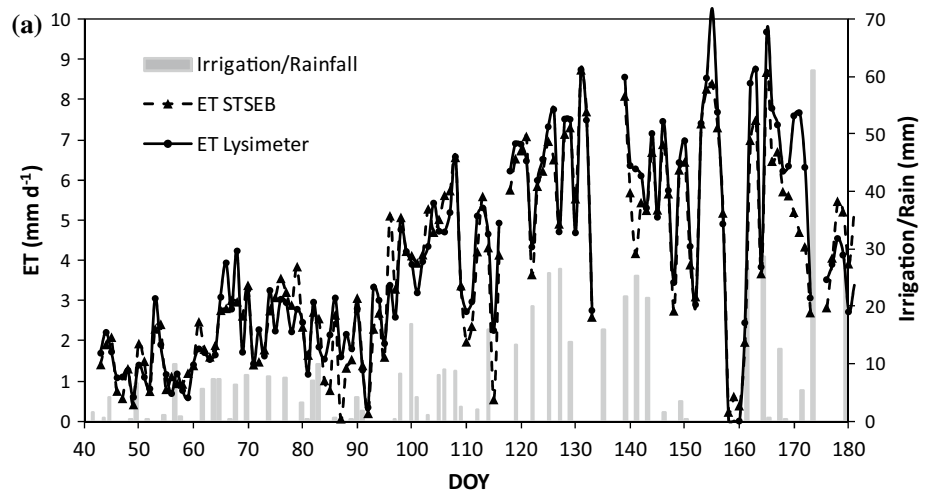

Fig. 6 Comparison of daily ET estimates with lysimeter measurements

Fig. 7 Cumulative values of predicted ET, *E*, and *T* values, for the whole wheat season, together with observed ET and irrigation + rain amount

simulations by the adjusted dual crop coefficients and results applying a water balance method. Yang et al. (2014) estimated daily ET using the EF method coupled with the daily net radiation, with an overall estimation error of

RMSE = ± 0.7 mm day^{-1} with a determination coefficient of 0.937. A daily average deviation of ± 0.9 mm day^{-1} was

obtained by Zhang et al. (2015) when comparing lysimeter measurements with estimations using an energy balance model together with MODIS data. In one of the very few ground-validated, ET studies at fine spatial scale for wheat, French et al. (2007) used airborne image observations as inputs in the TSEB model to calculate ET with accuracy to within ±1.3 mm day^{-1} for the full season, when compared to independent soil water depletion observations.

The total seasonal ET predicted by the STSEB model (500 mm) was <4 % lower than that measured in the lysimeter (520 mm) (see Fig. 7). Note that this agreement is particularly good for the initial stage (DOY < 90), when bare soil and low vegetation coverage conditions are traditionally a challenge for both energy and water balance models (Colaizzi et al. 2012; Shahrokhnia and Sepaskhah 2013).

Evaporation/transpiration partitioning

The E and T values calculated with the STSEB model using data from the present study are shown in Fig. 7. Soil E was clearly dominant for vegetation cover fractions below 0.2 (DOY < 90). The ratio T/E increased very fast, and T became the major contribution to ET after then. The total seasonal E resulted in 180 mm, with about half of this amount concentrated before DOY 90. Cumulative T value was 320 mm. This means 36 % of the seasonal wheat ET corresponds to soil evaporation. This modeled value is in agreement with former studies relative to wheat. López-Urrea et al. (2009) obtained a seasonal evaporation component amounting to 24 % (135 mm) of the total ET. Zhang et al. (2013) observed soil evaporation for winter wheat averaged 28 % during the full crop season, whereas it represented near 80 % for the initial stage and decreased to 5–6 % during the mid-season period. Sun et al. (2006) reported 30–35 % for non-stressed to mild-stressed winter wheat, and Sadras and Rodriguez (2010) reported 22–34 % in Australia. Using microlysimeters, Shahrokhnia and Sepaskhah (2013) estimated that soil evaporation was about 30 % of the total wheat ET. A lower ratio of 19 % was obtained for the seasonal E/ET of a winter wheat with a drip irrigation system (Gao et al. 2014). These findings should prompt further field studies of E and T partitioning for different irrigation systems and management strategies.

Crop coefficients

Figure 8a plots the curve of K_c calculated as the ratio of the lysimeter measured, and STSEB predictions, with the reference evapotranspiration (ET$_o$) calculated with the FAO-56 Penman–Monteith equation (Allen et al. 1998). K_c values are presented as 5-day averages to avoid the scatter produced by irrigation events. The average K_c data obtained from lysimeter measurements for each stage were: $K_{c\text{-ini}}$:

0.80, $K_{c\text{-mid}}$: 1.18, and $K_{c\text{-end}}$: 0.41, whereas the average K_c values obtained from STSEB calculations were: $K_{c\text{-ini}}$: 0.82, $K_{c\text{-mid}}$: 1.14, and $K_{c\text{-end}}$: 0.59. López-Urrea et al. (2009) reported similar behavior of K_c in a similar experiment over wheat in the same area using also lysimeter measurements. These authors reported wheat K_c values of $K_{c\text{-mid}}$: 1.20 and $K_{c\text{-end}}$: 0.15. The K_{c_mid} matched our measurements, whereas that difference in the $K_{c\text{-end}}$ is due to the higher values of ET at the end of this growth stage in our measurements, consequence of the relatively high value of $P_v = 0.23$ still present in DOY 180. Other authors obtained K_c values of 0.30–0.45 for $K_{c\text{-ini}}$, of 1.10–1.20 for $K_{c\text{-mid}}$, and $K_{c\text{-end}}$ in the range of 0.25–0.45 (Gontia and Tiwari 2010; Kjaersgaard et al. 2008; Howell et al. 2006; Allen et al. 1998). These $K_{c\text{-mid}}$ data are similar to our averaged $K_{c\text{-mid}}$, and small variations can be due to differences in: the planting date, lengths of growth stages, wheat varieties, cultural practices, and climatic conditions. Differences in the $K_{c\text{-ini}}$ and $K_{c\text{-end}}$ can be due to the higher values of evaporation during these two stages in our measurements. Shahrokhnia and Sepaskhah (2013) estimated values of 0.77, 1.35, and 0.26 for $K_{c\text{-ini}}$, $K_{c\text{-mid}}$, and $K_{c\text{-end}}$, respectively. Average $K_{c\text{-ini}}$ basically matched our measurements and $K_{c\text{-end}}$ was lower than our estimation, whereas our values of $K_{c\text{-mid}}$ were lower than those reported by these authors. These discrepancies could be due to different wheat varieties and climatic conditions as well as to eventual deviations in the reference ET calculations.

As stated by López-Urrea et al. (2009), soil evaporation component (E) can be significant when sprinkler system is used for irrigation or frequent rain events occur. This is the case of our study. Note the high values of $K_{c\text{-ini}}$ observed (Fig. 8a) for the initial stage of the wheat growing, with P_v values lower than 0.2.

Dual crop coefficients K_e and K_{cb} were calculated as the ratios E/ET$_o$ and T/ET$_o$, respectively. Figure 8b shows the comparison between results obtained and values proposed by FAO-56, all 5-day averaged. Relatively large values of K_e were obtained for establishment and the beginning of development stages due to frequent irrigations, while the vegetation cover was low. During reproduction, K_{cb} increased rapidly and peaked to 1.10 during the ripening stage. The average K_{cb} data obtained from STSEB calculations for each stage resulted in: $K_{cb\_ini} = 0.05$, $K_{cb\_mid} = 1.10$, and $K_{cb\text{-end}} = 0.19$. Modeled K_{cb} values were smaller than FAO-56 predictions. In terms of K_e, FAO-56 underestimated modeled values, particularly at the initial growth stage. Note that the K_e coefficient is greatly affected by irrigation strategy, soil type, canopy coverage, and local weather conditions.

Zhang et al. (2013) estimated initial, mid-season, and end K_{cb} values for wheat of 0.25, 1.15, and 0.30, respectively. Similar values were obtained by Shahrokhnia and

Fig. 8 Comparison of modeled values of crop coefficients with those calculated from lysimeter measurements and proposed by FAO-56: **a** K_c, **b** K_e, and K_{cb}
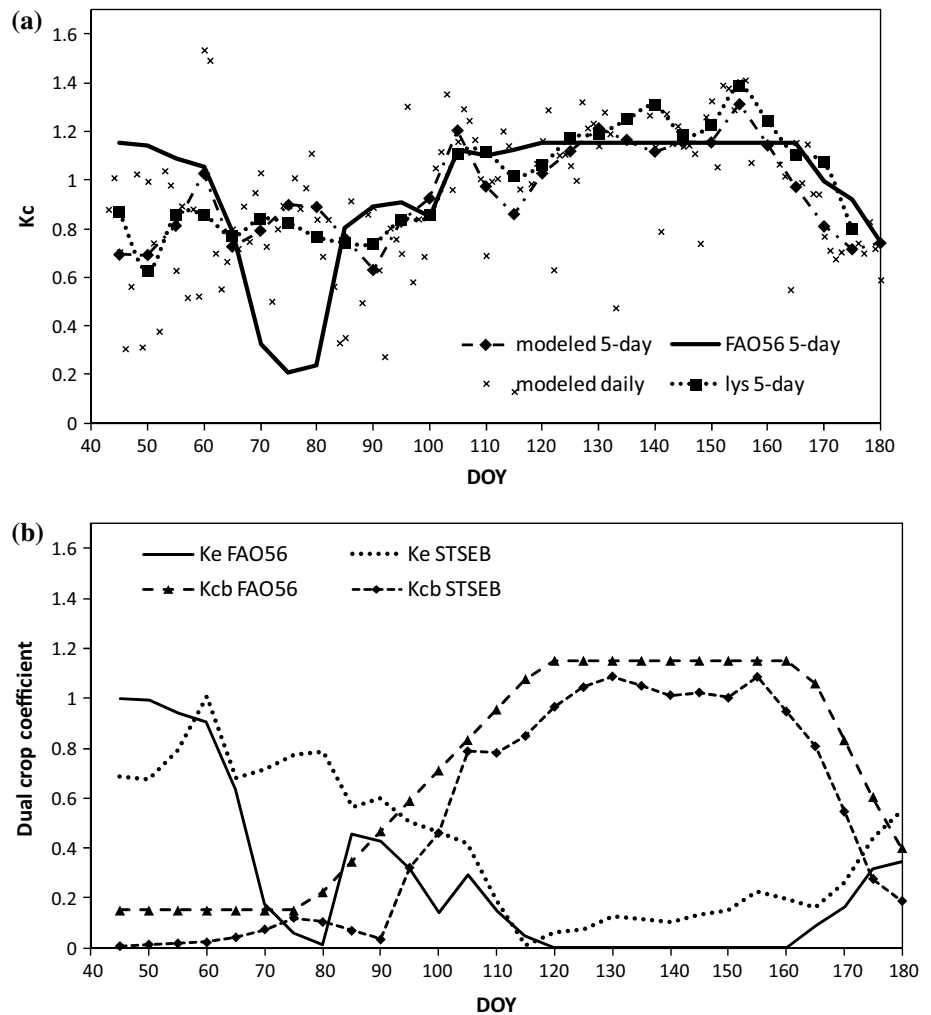
Sepaskhah (2013), ranging between 0.18–0.27, 1.11–1.16, and 0.11–0.14 for initial, mid-, and end-season stages, respectively. Gao et al. (2014) also obtained K_{cb} values ranging 0.22–0.27, 1.02–1.10, and 0.25–0.43, for initial, mid-, and end-season stages, respectively, in subsurface drip-irrigated wheat. All these reported $K_{cb\text{-}mid}$ and $K_{cb\text{-}end}$ values are in agreement with our estimates, whereas those observed $K_{cb\text{-}ini}$ values from previous studies are clearly larger than our predicted average $K_{cb\text{-}ini}$. Differences at this point are likely due to a higher canopy cover during the initial growth stage in the studies reported in the literature.

Conclusions

Results in this paper reinforce the potential of the techniques based on the combination of surface energy balance with radiometric temperatures for irrigation scheduling or water management under a variety of crops and surface conditions.

In this work, we focused on a spring wheat crop located in a semiarid region of central Spain. Comparison between model estimates and lysimeter measurements showed a RMSE value of ±0.8 mm day^{-1}, in agreement with previous results using the same technique over sorghum, sunflower, or canola. Furthermore, this error is maintained for more than 80 % of the 130 days of the experiment duration and equally for all vegetation cover conditions. Accuracy improves when cumulative ET values are calculated. A deviation no greater than 4 % (20 mm) is observed for the prediction of the total 520 mm measured for the full wheat growing season.

Partition of ET into E and T components resulted in 36 % of the total ET corresponding to the soil evaporation, although most of it was concentrated in the initial phase ($P_v < 0.4$). A proper implementation of the STSEB approach might become a useful tool at this point when facing strategies to increase crop water use efficiency through a feasible monitoring of the soil evaporation/transpiration partitioning.

Crop coefficient and dual crop coefficients were also computed. Results are in agreement with those K_c obtained from the lysimeter measurements, and the K_{cb}, and K_e values shown by other authors for wheat. This technique could be used for the local adjustment of the FAO-56 K_c values, as an alternative in those fields where weighing lysimeters are not available.

The main limitation for the operational application of the energy balance modeling at a crop field scale is the coarse spatial resolution of the thermal data provided by the orbiting satellites. Recent advances in downscaling TIR information from low–medium spatial resolution sensors, using VIS/NIR medium–high spatial resolution sensors, bring the opportunity to the operational application of the technique presented from satellite data. With this aim, a modified STSEB-T_R approach was presented. This version was conceived to be applied using the composite target temperature T_R as the unique radiometric temperature input. Results using this new formulation match those using the original STSEB model, under the conditions of the present study. Further work is required, including evaporation and transpiration measurements under different field and environmental conditions, before extracting any firm conclusion at this point.

Compliance with ethical standards

Conflicts of interest The authors declare no conflict of interest.

Appendix

The original formulation of the simplified two-source energy balance model (STSEB) (Sánchez et al. 2008) used the measured temperature of both soil (T_s) and canopy (T_c) components to calculate the different terms of the energy balance equation:

$$R_n = H + ET + G \tag{1}$$

where R_n is the net radiation flux (W m^{-2}), H is the sensible heat flux (W m^{-2}), ET is the latent heat flux (W m^{-2}), and G is the soil heat flux (W m^{-2}).

According to the STSEB approach, the sum of the soil and canopy contributions (values per unit area of component) to the total sensible heat flux, H_s and H_c, respectively, are weighted by their respective partial areas as follows:

$$H = P_v H_c + (1 - P_v) H_s \tag{2}$$

where P_v is the vegetation cover fraction at nadir. In Eq. (2), H_s and H_c are expressed as:

$$H_c = \rho C_p \frac{T_c - T_a}{r_a^h} \tag{3a}$$

$$H_s = \rho C_p \frac{T_s - T_a}{r_a^a + r_a^s} \tag{3b}$$

where ρC_p is the volumetric heat capacity of air (J K^{-1}m^{-3}), T_a is the air temperature at a reference height (h), r_a^h is the aerodynamic resistance to heat transfer between the canopy and the reference height at which the atmospheric data are measured (s m^{-1}), r_a^a is the aerodynamic resistance to heat transfer between the point $z_{0M} + d$ (z_{0M}: canopy roughness length for momentum, d: displacement height) and the reference height (s m^{-1}), and r_a^s is the aerodynamic resistance to heat flow in the boundary layer immediately above the soil surface (s m^{-1}). A summary of the expressions to estimate these resistances can be found in Sánchez et al. (2008). Equations (3a) and (3b) are taken from the parallel configuration of the TSEB model (Norman et al. 1995; Li et al. 2005), modified to take into account the distinction between r_a^h and r_a^a (Sánchez et al. 2008).

The partitioning of the net radiation flux, R_n, between the soil and canopy is proposed as follows:

$$R_n = P_v R_{nc} + (1 - P_v) R_{ns} \tag{4}$$

where R_{nc} and R_{ns} are the contributions (values per unit area of component) of the canopy and soil, respectively, to the total net radiation flux. They are estimated by establishing a balance between the long-wave and the short-wave radiation separately for each component:

$$R_{nc} = (1 - \alpha_c)S + \varepsilon_c L_{sky} - \varepsilon_c \sigma T_c^4 \tag{5a}$$

$$R_{ns} = (1 - \alpha_s)S + \varepsilon_s L_{sky} - \varepsilon_s \sigma T_s^4 \tag{5b}$$

where S is the solar global radiation (W m^{-2}), α_s and α_c are soil and canopy albedos, respectively, σ is the Stefan–Boltzmann constant, and L_{sky} is the incident long-wave radiation (W m^{-2}).

A similar expression is used to combine the soil and canopy contributions, ET_s and ET_c, respectively, to the total latent heat flux:

$$ET = P_v ET_c + (1 - P_v) ET_s \tag{6}$$

According to this framework, a complete and independent energy balance between the atmosphere and each component of the surface is established from the assumption that all the fluxes act vertically. In this way, the component fluxes to the total latent heat flux can be written as:

$$ET_c = R_{nc} - H_c \tag{7a}$$

$$\mathrm{ET_s} = R_{\mathrm{ns}} - H_{\mathrm{s}} - \frac{G}{(1 - P_{\mathrm{v}})} \tag{7b}$$

Finally, G can be estimated as a fraction (C_{G}) of the soil contribution to the net radiation (Choudhury et al. 1987):

$$G = C_{\mathrm{G}}(1 - P_{\mathrm{v}})R_{\mathrm{ns}} \tag{8}$$

where C_{G} can vary in a range of 0.2–0.5 depending on the soil type and moisture. A value of $C_{\mathrm{G}} = 0.35$ was used in this work.

When the composed target temperature (T_{R}) is the only measurement available, the original formulation of the STSEB needs the inclusion of additional assumptions to calculate, for example, an initial estimate of canopy latent heat flux. In this STSEB-T_{R} approach, the Priestley–Taylor equation was used:

$$\mathrm{ET_c} = f_{\mathrm{g}}\alpha \left[\frac{\Delta}{\Delta + \gamma} \right] R_{\mathrm{nc}} \tag{9}$$

where f_{g} is the fraction of the vegetation that is green, Δ is the slope of the water vapor saturation curve, α is the Priestley–Taylor (PT) parameter (Priestley and Taylor 1972), and γ is the psychrometric constant. A value of $\alpha = 1.26$ was assumed in this study, according to the non-water-stressed conditions over this wheat field (French et al. 2007). Note that this value might need adjustment under water-stressed conditions.

An initial value of T_{c} is extracted by solving the equation resulting from the combination of (5a), (7a), and (9). Then, the corresponding value of T_{s} can be calculated from the equation (Sánchez et al. 2008):

$$\varepsilon T_{\mathrm{R}}^4 = P_{\mathrm{v}}\varepsilon_{\mathrm{c}}T_{\mathrm{c}}^4 + (1 - P_{\mathrm{v}})\varepsilon_{\mathrm{s}}T_{\mathrm{s}}^4 \tag{10}$$

where ε_{c} and ε_{s} are the canopy and soil emissivities, respectively, ε is the effective surface emissivity. Once T_{c} and T_{s} values are estimated, Eqs. (2)–(8) can be applied.

References

Agam N, Kustas WP, Anderson MC, Li F, Neale CN (2007) A vegetation index based technique for spatial sharpening of thermal imagery. Remote Sens Environ 107:545–558

Allen RG, Pereira LS, Raes D, Smith M (1998) Crop evapotranspiration: guidelines for computing crop water requirements. In: Proceedings of the FAO irrigation and drainage paper no. 56. Roma, Italy

Bindhu VM, Narasimhan B, Sudheer KP (2013) Development and verification of a non-linear disaggregation method (NL-DisTrad) to downscale MODIS land surface temperature to the spatial scale of Landsat thermal data to estimate evapotranspiration. Remote Sens Environ 135:118–129

Calera A, Martínez C, Melia J (2001) A procedure for obtaining green plant cover: relation to NDVI in a case study for barley. Int J Remote Sens 22:3357–3362

Campos I, Neale CMU, Calera A, Balbontín C (2010) Assessing satellite-based basal crop coefficients for irrigated grapes (*Vitis vinífera* L.). Agric Water Manag 98:45–54

Choudhury BJ, Idso SB, Reginato RJ (1987) Analysis of an empirical model for soil heat flux under a growing wheat crop for estimating evaporation by an infrared-temperature based energy balance equation. Agric For Meteorol 39:283–297

Cihlar J, Dobson MC, Schmugge T, Hoogeboom P, Janse ARP, Baret F, Guyot G, Le Toan T, Pampaloni P (1987) Procedures for the description of agricultural crops and soils in optical and microwave remote sensing studies. Int J Remote Sens 8:427–439

Colaizzi PD, Kustas WP, Anderson MC, Agam N, Tolk JA, Evett SR, Howell TA, Gowda PH, O´Shaughnessy SA (2012) Two-source energy balance model estimates of evapotranspiration using component and composite surface temperatures. Adv Water Res 50:134–151

FAO (2014) FAO Statistical Database (online). Consultation: January 20, 2014. http://faostat3.fao.org/home/E

Farg E, Arafat SM, Abd El-Wahed MS, El-Gindy AM (2012) Estimation of Evapotranspiration ETc and crop coefficient Kc of wheat, in south Nile Delta of Egypt using integrated FAO-56 approach and remote sensing data. Egypt J Remote Sens Space Sci 15:83–89

French AN, Hunsaker DJ, Clarke TR, Fitzgerald GJ, Luckett WE, Pinter PJ (2007) Energy balance estimation of evapotranspiration for wheat grown under variable management practices in Central Arizona. Trans ASABE 50(6):2059–2071

Gao F, Kustas WP, Anderson MC (2012) A data mining approach for sharpening thermal satellite imagery over land. Remote Sens 4:3287–3319

Gao Y, Yang L, Shen X, Li X, Sun J, Duan A, Wu L (2014) Winter wheat with subsurface drip irrigation (SDI): crop coefficients, water-use estimates, and effects of SDI on grain yield and water use efficiency. Agric Water Manag 146:1–10

Ghamarnia H, Miri E, Ghobadei M (2014) Determination of water requirement, single and dual crop coefficients of black cumin (*Nigella sativa L.*) in a semi-arid climate. Irrig Sci 32(1):67–76

Gontia NK, Tiwari KN (2010) Estimation of crop coefficient and evapotranspiration of wheat (*Triticum aestivum*) in an irrigation command using remote sensing and GIS. Water Resour Manag 24:1399–1414

Howell TA, Schneider AD, Dusek DA, Marek TH, Steiner JL (1995) Calibration and scale performance of Bushland weighing lysimeters. Trans ASAE 38(4):1019–1024

Howell TA, Evett SR, Tolk JA, Copeland KS, Dusek DA, Colaizzi PD (2006) Crop coefficients developed at Bushland, Texas for corn, wheat, sorghum, soybean, cotton, and alfalfa. In: Proceeding of the world environmental and water resources congress, Omaha, NE, p 9

Howell TA, Evett SR, Tolk JA, Copelan KS, Marek TH (2012) Evapotranspiration and crop coefficients for irrigated sunflower in the Southern High Plains. ASABE paper no. 12-1338306. ASABE, St. Joseph

Hunsaker DJ, Pinter PJ Jr, Kimball BA (2005) Wheat basal crop coefficients determined by normalized difference vegetation index. Irrig Sci 24(1):1–14

Kjaersgaard JH, Plauborg FL, Mollerup M, Petersen CT, Hansen S (2008) Crop coefficients for winter wheat in a sub-humid climate regime. Agric Water Manag 95:918–924

Kustas WP, Alfieri JG, Anderson MC, Colaizzi PD, Prueger JH, Evett SR, Neale CMU, French AN, Hipps LE, Chávez JL, Copeland KS, Howell TA (2012) Evaluating the two-source energy balance model using local thermal and surface flux observations in a strongly advective irrigated agricultural area. Adv Water Res 50:120–133

Li F, Kustas WP, Prueger JH, Diak GR (2005) Utility of remote sensing based two-source energy balance model under low and high vegetation cover conditions. J Hydrometeorol 6:878–891

López-Urrea R, de Santa Martín, Olalla F, Fabeiro C, Moratalla A (2006) Testing evapotranspiration equations using lysimeter observations in a semiarid climate. Agric Water Manag 85:15–26

López-Urrea R, Montoro A, González-Piqueras J, López-Fuster P, Fereres E (2009) Water use of spring wheat to raise water productivity. Agric Water Manag 96:1305–1310

López-Urrea R, Montoro A, Mañas F, López-Fuster P, Fereres E (2012) Evapotranspiration and crop coefficients from lysimeter measurements of mature 'Tempranillo' wine grapes. Agric Water Manage 112:13–20

López-Urrea R, Montoro A, Trout TJ (2014) Consumptive water use and crop coefficients of irrigated sunflower. Irrig Sci 32(2):99–109

MAGRAMA (2014) Anuario de Estadística 2013. Ministerio de Agricultura, Alimentación y Medio Ambiente, Madrid, p 1095

Norman JM, Kustas WP, Humes KS (1995) A two-source approach for estimating soil and vegetation energy fluxes from observations of directional radiometric surface temperature. Agric For Meteorol 77:263–293

Priestley CHB, Taylor RJ (1972) On the assessment of surface heat flux and evaporation using large-scale parameters. Mon Weather Rev 100:81–92

Rubio E, Caselles V, Coll C, Valor E, Sospedra F (2003) Thermal-infrared emissivities of natural surfaces: improvements on the experimental set-up and new measurements. Int J Remote Sens 24:5379–5390

Sadras VO, Rodriguez D (2010) Modelling the nitrogen-driven tradeoff between nitrogen utilisation efficiency and water use efficiency of wheat in eastern Australia. Field Crops Res 118:297–305

Sánchez JM, Kustas WP, Caselles V, Anderson M (2008) Modelling surface energy fluxes over maize using a two-source patch model and radiometric soil and canopy temperature observations. Remote Sens Environ 112:1130–1143

Sánchez JM, López-Urrea R, Rubio E, Caselles V (2011) Determining water use of sorghum from two-source energy balance and radiometric temperatures. Hydrol Earth Syst Sci 15:3061–3070

Sánchez JM, López-Urrea R, Rubio E, González-Piqueras J, Caselles V (2014) Assessing crop coefficients of sunflower and canola using two-source energy balance and thermal radiometry. Agric Water Manag 137:23–29

Shahrokhnia MH, Sepaskhah AR (2013) Single and dual crop coefficient and crop evapotranspiration for wheat and maize in a semi-arid region. Theor Appl Climatol 114:495–510

Sun HY, Liu CM, Zhang XY, Shen YJ, Zhang YQ (2006) Effects of irrigation on water balance, yield and WUE of winter wheat in the North China Plain. Agric Water Manag 85:211–218

Williams LE, Ayars JE (2005) Grapevine water use and the crop coefficient are linear functions of the shaded area measured beneath the canopy. Agric For Meteorol 132:201–211

Willmott CJ (1982) Some comments on the evaluation of model performance. Bull Am Meteorol Soc 63(11):1309–1313

Yang G, Pu R, Zhao Ch, Xue X (2014) Estimating high spatiotemporal resolution evapotranspiration over a winter wheat field using an IKONOS image based complementary relationship and Lysimeter observations. Agric Water Manag 133:34–43

Zhang B, Liu Y, Xu D, Zhao N, Lei B, Rosa RD, Paredes P, Paço TA, Pereira LS (2013) The dual crop coefficient approach to estimate and partitioning evapotranspiration of the winter wheat-summer maize crop sequence in North China Plain. Irrig Sci 31:1303–1316

Zhang S, Zhao H, Lei H, Shao H, Liu T (2015) Winter wheat productivity evaluated by the developed remote sensing evapotranspiration model in Hebei Plain, China. Sci World J 2015:384086-1–384086-10. doi:10.1155/2015/384086

Zhao N, Liu Y, Cai J, Paredes P, Rosa RD, Pereira LS (2013) Dual crop coefficient modelling applied to the winter wheat-summer maize crop sequence in North China Plain: basal crop coefficients and soil evaporation component. Agric Water Manag 117:93–105